


ARTICLE OPEN



Role of liver FGF21-KLB signaling in ketogenic diet-induced amelioration of hepatic steatosis

Wanrong Guo^{1,2,3,4,8}, Huanyi Cao^{2,5,8}, Yunfeng Shen⁶, Wuguo Li⁷, Wei Wang^{2,6}, Lidan Cheng^{2,6}, Mengyin Cai^{1,2,3} and Fen Xu^{1,2,3} 

© The Author(s) 2024

BACKGROUND: The effectiveness of ketogenic diet (KD) in ameliorating fatty liver has been established, although its mechanism is under investigation. Fibroblast growth factor 21 (FGF21) positively regulates obesity-associated metabolic disorders and is elevated by KD. FGF21 conventionally initiates its intracellular signaling via receptor β -klotho (KLB). However, the mechanistic role of FGF21-KLB signaling for KD-ameliorated fatty liver remains unknown. This study aimed to delineate the critical role of FGF21 signaling in the ameliorative effects of KD on hepatic steatosis.

METHODS: Eight-week-old C57BL/6 J mice were fed a chow diet (CD), a high-fat diet (HFD), or a KD for 16 weeks. Adeno-associated virus-mediated liver-specific KLB knockdown mice and control mice were fed a KD for 16 weeks. Phenotypic assessments were conducted during and after the intervention. We investigated the mechanism underlying KD-alleviated hepatic steatosis using multi-omics and validated the expression of key genes.

RESULTS: KD improved hepatic steatosis by upregulating fatty acid oxidation and downregulating lipogenesis. Transcriptional analysis revealed that KD dramatically activated FGF21 pathway, including KLB and fibroblast growth factor receptor 1 (FGFR1). Impairing liver FGF21 signaling via KLB knockdown diminished the beneficial effects of KD on ameliorating fatty liver, insulin resistance, and regulating lipid metabolism.

CONCLUSION: KD demonstrates beneficial effects on diet-induced metabolic disorders, particularly on hepatic steatosis. Liver FGF21-KLB signaling plays a critical role in the KD-induced amelioration of hepatic steatosis.

Nutrition and Diabetes (2024)14:18; <https://doi.org/10.1038/s41387-024-00277-3>

INTRODUCTION

Non-alcoholic fatty liver disease (NAFLD) stands as one of the most common chronic liver diseases globally, with an estimated prevalence of 32.4% [1]. Lifestyle interventions, including dietary adjustments and physical activity, are the main recommendations for managing NAFLD. Within this context, caloric intake, dietary composition, and meal timing have emerged as focal points in NAFLD treatment [2].

The ketogenic diet (KD), initially developed for epilepsy treatment, is characterized by a composition with over 90% of calories from fat and less than 1% of calories from carbohydrates [3]. Clinical studies have demonstrated that KD induced a remarkable reduction in body weight and the amelioration of fatty liver, accompanied by decreased alanine aminotransferase and aspartate aminotransferase levels [4–6]. Rodent models fed a KD have showcased weight loss, improved insulin sensitivity, lipid metabolism, and glucose metabolism [7–10]. In hepatology studies, KD has been noted to enhance hepatic energy expenditure, promote fatty acid oxidation, and suppress lipogenesis compared with high-fat diets (HFD) or western diets [7, 8].

Mechanistically, KD activates AMP-activated protein kinase and inhibits acetyl-CoA carboxylase (ACC) activity in the liver and muscle [7]. Moreover, our previous study has elucidated that KD reduces malonylation of acetyl-CoA carboxylase 1 (ACC1), critical for activity and stability of ACC1, thereby alleviating fatty liver [11]. Besides the liver, KD activates brown adipose tissue (BAT) function by upregulating heat-related gene expression [12] and mitigates inflammation in white adipose tissues (WATs) [13].

Fibroblast growth factor 21 (FGF21), a crucial metabolic regulator primarily synthesized in the liver, modulates the metabolism of multiple tissues [14]. Elevating serum FGF21 levels through exogenous administration or liver overexpression induces weight loss, enhances energy expenditure, improves glucose metabolism and insulin sensitivity, alleviates hepatic steatosis, promotes lipolysis, induces browning of WAT, and activates BAT function [15–21]. A phase 2a clinical trial has further validated the beneficial effects of FGF21 on steatohepatitis [22].

FGF21 is upregulated by KD [23, 24]. FGF21-deficient mice fed a KD gained weight and developed hepatic steatosis, whereas control mice exhibited weight loss and reduced fatty liver [25].

¹Department of Endocrinology and Metabolism, The Third Affiliated Hospital of Sun Yat-sen University, Guangzhou, China. ²Guangdong Provincial Key Laboratory of Diabetology, Guangzhou, China. ³Guangzhou Municipal Key Laboratory of Mechanistic and Translational Obesity Research, The Third Affiliated Hospital of Sun Yat-sen University, Guangzhou, China. ⁴Medical Intensive Care Unit, The Third Affiliated Hospital of Sun Yat-sen University, Guangzhou, China. ⁵Department of Endocrinology, Guangdong Provincial People's Hospital, Guangdong Academy of Medical Sciences, Southern Medical University, Guangzhou, China. ⁶Department of Endocrinology and Metabolism, The Second Affiliated Hospital of Nanchang University, Nanchang, China. ⁷Animal Experiment Center, The First Affiliated Hospital of Sun Yat-sen University, Guangzhou, China. ⁸These authors contributed equally: Wanrong Guo, Huanyi Cao. ✉email: xufen3@mail.sysu.edu.cn

Received: 21 October 2023 Revised: 1 April 2024 Accepted: 4 April 2024

Published online: 12 April 2024

Liver-specific FGF21-knockdown mice fed a KD also displayed fatty liver compared with control mice [23]. FGF21 signals target cells through a receptor complex composed of FGF receptor (FGFR), FGFR1c, and a co-receptor called β -klotho (KLB). Elimination of either FGFR1 or KLB impairs the acute insulin-sensitizing effects of FGF21 [26, 27]. Thus, we hypothesized that KD might ameliorate hepatic steatosis via hepatic FGF21-KLB signaling. In this study, we aimed to delineate the critical role of FGF21 signaling in the ameliorative effects of KD on hepatic steatosis in order to offer new insights into the potential of KD in the treatment of NAFLD.

MATERIALS AND METHODS

Animal experiments

Seven-week-old male C57BL/6J mice were purchased from GemPharmatech (Nanjing, China). Mice were housed in a standard specific pathogen-free facility with free access to food and water. After a 1-week acclimatization period, eight-week-old mice were used in two experiments. In the first experiment, mice were divided randomly into three groups ($n = 5$ per group), which were exposed to a chow diet (CD, 11% fat [kcal%]; Guangdong Medical Laboratory Animal Center, Guangzhou, China), an HFD (58% fat [kcal%]; D12331; Research Diets, New Brunswick, NJ, USA), or an HFD and a ketogenic diet (KD, 90.5% fat [kcal%], TD.160153, Envigo, USA) alternating every 2 weeks for a total period of 16 weeks. In the second experiment, adeno-associated virus (AAV) expressing short-hairpin RNAs targeting β -klotho (*shKlb*) and negative control (*shCtrl*) were administered to generate liver-specific KLB knockdown mice and control mice, and then mice were subjected to 16-week diet intervention on the next day. Body weight, blood glucose, and food intake were recorded every 2 weeks. Blood and tissue samples were collected after overnight fasting. All animal experiments complied with the ARRIVE guidelines and were approved by the Institutional Animal Care and Use Committee of Sun Yat-sen University.

AAV9-mediated gene knockdown

AAVs expressing *shKlb* (5'-GCAATCTGTCCAAAGTTAACA-3') and *shCtrl* were purchased from Genechem Co., Ltd (Shanghai, China). The sequence was validated in a previous study to effectively knock down *Klb* expression in mouse liver [20]. AAV9 (1.0×10^{11} active viral particles/mouse) was injected via the tail vein to suppress *Klb* expression in the liver.

Body composition measurement

After the dietary exposure, body composition was measured by a quantitative magnetic resonance EchoMRI™-100 (EchoMRI LLC, Houston, TX, USA) consciously according to the manufacturer's instructions. Mice were carefully fixed in tubes and then inserted into the EchoMRI™-100 machine one at a time, and fat and lean masses were analyzed and recorded by the machine within 1 min. Fat mass is presented as the ratio to body weight.

Glucose and insulin tolerance tests

Glucose tolerance test was performed in overnight-fasted mice by intraperitoneally injecting with glucose (2.0 g/kg body weight). Blood samples were collected for serum insulin measurement. For the insulin tolerance test, the mice were intraperitoneally injected with insulin (0.65 units/kg body weight, Novolin R, Novo Nordisk Inc., Denmark) after 6 h of fasting. Blood glucose levels were recorded at various time points after the injection.

Biochemical and immunological analyses

Triglycerides, total cholesterol, and free fatty acids were quantified using commercial kits (triglycerides, K622-100; cholesterol, K603-100; free fatty acids, K612-100; Biovision, Milpitas, CA, USA). Serum insulin concentration was measured with an ELISA kit (#10-1247-01; Mercodia, Uppsala, Sweden), and another commercial kit (#32180; Immunodiagnosics Limited, Science Park, Hong Kong, China) was used in FGF21 measurement. Every sample was assayed in duplicate.

Hematoxylin and eosin staining

Hematoxylin and eosin staining was performed according to standard procedures [28]. Fresh tissues were fixed in 4% paraformaldehyde solution

(GBCBIO, Guangzhou, China) at 4°C overnight. Then, tissues were embedded in paraffin and sectioned at 3–5 μ m at room temperature. The sections were deparaffinized twice with fresh xylene and dehydrated with ethanol at a gradient concentration. Next, the nucleus was stained with hematoxylin, and the cytoplasm was stained with eosin. Photomicrographs were obtained using a DMI8 inverted microscope (Leica Microsystems, Wetzlar, Germany).

Oil Red O staining

Oil Red O staining was performed according to standard procedures [28, 29]. Briefly, fresh liver tissues were embedded in OCT compound (Sakura Finetek, Torrance, CA, USA) and stored at -80°C . Liver tissues were next sectioned at 6–8 μ m at -18°C and washed with 60% isopropanol. A stock solution was prepared using Oil Red O powder (O0625; Sigma Aldrich, St Louis, MO, USA) dissolved in isopropanol and protected from light; a working concentration of 60% was diluted with ddH₂O. The sections were stained with Oil Red O working solution for 1 h and washed under running tap water for 20 min. After Oil Red O staining, tissue sections were counterstained with hematoxylin for 1 min. The Oil Red O staining procedure was performed in the dark. Photomicrographs were obtained using a DMI8 inverted microscope (Leica Microsystems).

Real-time qPCR

Total RNA was extracted from frozen tissues using Trizol Reagent (Sigma Aldrich) [30]. cDNA was synthesized from the RNA by reverse transcription using a Transcriptor First Strand cDNA Synthesis Kit (Roche Applied Science, Basel, Switzerland). Real-time PCR was performed using a LightCycler 480 System with LightCycler 480 SYBR Green Master Mix (Roche Applied Science). Target gene expression was normalized against β -actin, and the fold change in mRNA expression was determined using the $2^{-\Delta\Delta\text{CT}}$ method.

Western blotting

Protein was extracted from tissues using RIPA lysis and extraction buffer (89900; Thermo Fisher Scientific, Waltham, MA, USA) combined with Halt™ Protease and Phosphatase Inhibitor Cocktail (78440; Thermo Fisher Scientific). Next, an equal amount (30 μ g) of protein was separated by 10% SDS-PAGE and transferred onto a polyvinylidene fluoride membrane (EMD Millipore, Burlington, MA, USA). Membranes were incubated with 0.1% (1:1000) target primary antibodies at 4°C overnight and then with 0.01% (1:10000) secondary antibodies at room temperature for 1 h protected from light. After washing thrice with TBS, the protein bands were visualized using the Odyssey Infrared Imaging System (LI-COR, Nebraska, USA). Antibodies against acetyl-CoA carboxylase (ACC) (3676 S), fatty acid synthase (FASN) (3180 S), stearyl-coenzyme A desaturase 1 (SCD1) (2794 S), and β -actin (4970 s) were purchased from Cell Signaling Technology (Danvers, MA, USA). Fibroblast growth factor receptor 1 (FGFR1) (60325-1-Ig) antibody was purchased from Proteintech (Wuhan, China). Carnitine palmitoyltransferase 1 α (CPT1 α) antibody (sc-31128) was purchased from Santa Cruz Biotechnology (Dallas, TX, USA). KLB antibody (AF-2619) was purchased from R&D System (Minneapolis, MN, USA).

Immunofluorescence staining

Immunofluorescence staining of mouse livers was performed as previously described [11]. Tissue sections were prepared for hematoxylin and eosin staining as previously described. Sections were immersed in preheated citrate buffer and blocked with 3% hydrogen peroxide. Primary antibodies (0.5%, 1:200) against ACC, FASN, CPT1 α , FGFR1, and KLB were applied to the sections overnight at 4°C, followed by incubation with secondary antibodies (0.2%, 1:500). Finally, the nuclei were stained with DAPI for 10 min and washed with PBS. Photomicrographs were obtained using a DMI8 inverted microscope and Leica Qwin image analysis software (Leica Microsystems).

RNA sequencing

Total RNA was extracted from fresh mouse livers using an RNeasy Plus Mini kit (QIAGEN, Hilden, Germany) according to the manufacturer's instructions. An Agilent 2100 Bioanalyzer System (Agilent Technologies, Palo Alto, CA, USA) and Agilent RNA 6000 Nano Kit (Agilent Technologies) were used to assess the integrity and concentration of total RNA. Samples with an RNA integrity number >8 were considered suitable for further analyses. RNA sequencing and data analysis (GEO: GSE226139) were conducted by

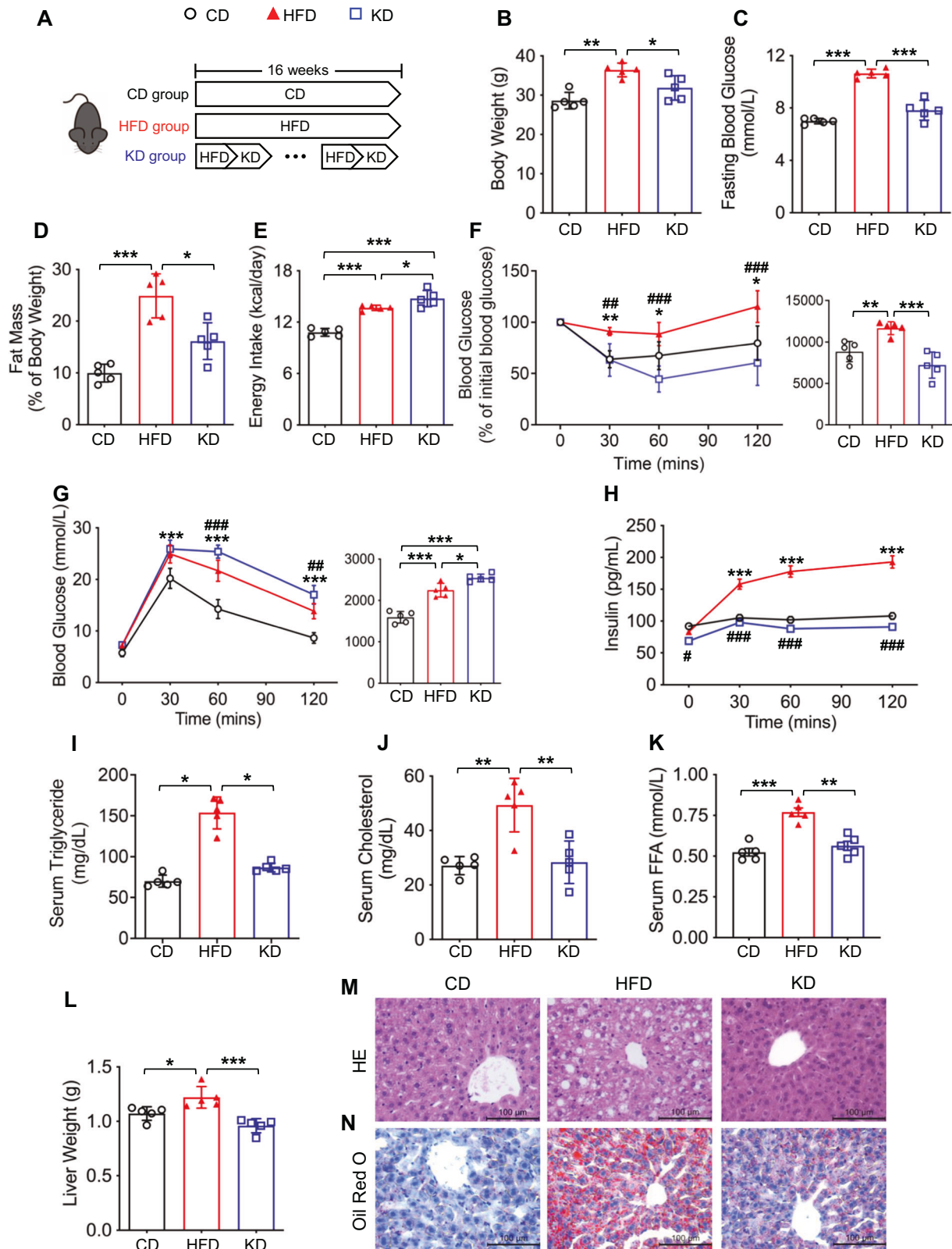


Fig. 1 KD ameliorates HFD-induced adiposity and fatty liver. **A** Procedure of the animal experiment. **B** Body weight. **C** Fasting blood glucose. **D** Fat mass-to-body weight ratio. **E** Energy intake. **F** Intrapерitoneal insulin tolerance test. **G** Intrapерitoneal glucose tolerance test. **H** Intrapерitoneal insulin release test. **I** Serum triglyceride level. **J** Serum cholesterol level. **K** Serum free fatty acid level. **L** Liver weight. **M** Hematoxylin and eosin staining of the liver (magnification 400x, scale bar, 100 μm). **N** Oil Red O staining of the liver (magnification 400x, scale bar, 100 μm). CD, chow diet; HFD, high-fat diet; KD, ketogenic diet. n = 5 mice per group. * $P < 0.05$; ** $P < 0.01$; *** $P < 0.001$. Line chart: * $P < 0.05$, ** $P < 0.01$, *** $P < 0.001$, HFD group vs CD group; # $P < 0.05$, ## $P < 0.01$, ### $P < 0.001$, KD group vs HFD group.

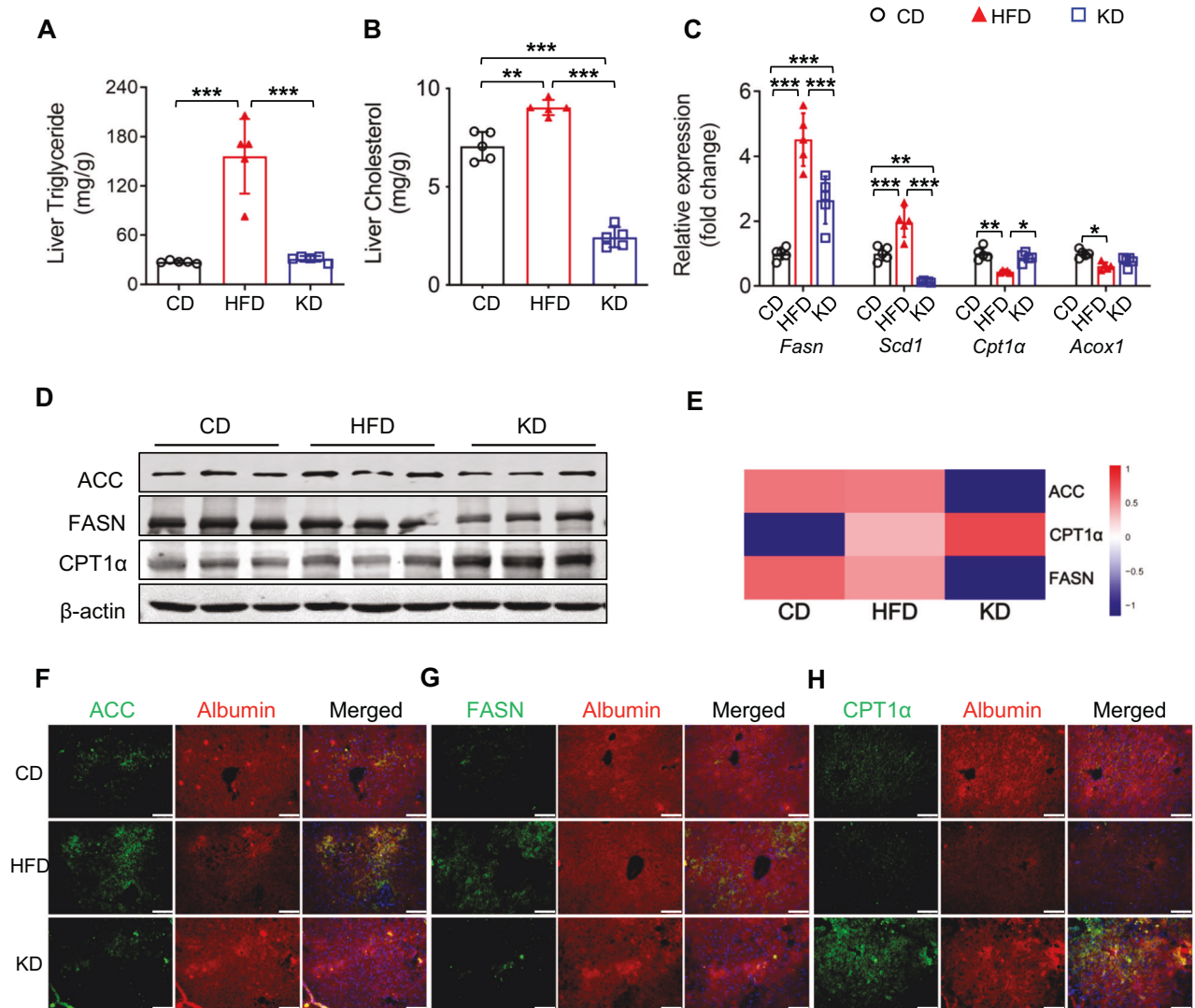


Fig. 2 KD activates hepatic fatty acid oxidation and suppresses lipogenesis. **A** Liver triglyceride level. **B** Liver cholesterol level. **C** mRNA expression of genes related to lipid metabolism in the liver. **D** Lipid metabolism related protein levels in the liver. **E** Heatmap of differentially expressed proteins related to lipid metabolism in the liver. Blue, downregulation; red, upregulation. **F–H** Immunofluorescence staining of albumin, ACC, FASN, and CPT1 α in the liver. Green, ACC **F**, FASN **G**, and CPT1 α **H**; red, albumin; blue, DAPI (magnification 200 \times , scale bar, 100 μ m). ACC, acetyl-CoA carboxylase; FASN, fatty acid synthase; CPT1 α , carnitine palmitoyltransferase 1 α ; *Acox1*, acyl-CoA oxidase 1. $n = 5$ mice per group. * $P < 0.05$; ** $P < 0.01$; *** $P < 0.001$.

Pan-Guarantee Biotechnology Co., Ltd (Guangzhou, China), as previously described [11].

Proteomic analysis

Proteins from mouse livers were isolated using a lysis buffer (8 mol/L urea, 1% protease inhibitor cocktail, 3 mmol/L trichostatin A, and 50 mmol/L nicotinamide), followed by sonication using a high-intensity ultrasonic processor (Scientz Biotechnology, Ningbo, China) and centrifugation. A BCA kit (Thermo Fisher Scientific) was used to measure the protein concentration according to the manufacturer's instructions. Proteomic analysis (PRIDE: PXD040481) was performed using the Jingjie PTM Bio-Labs (Hangzhou, China) as previously described [11].

Statistical analyses

Data are presented as mean \pm standard deviation. Statistical analysis was performed using SPSS 20.0 (IBM, USA). Unpaired two-tailed t-test was used in comparing differences between two groups, and one-way analysis of variance was used in calculating differences among the three groups with the least significant difference test. Statistical significance was set at $P < 0.05$.

RESULTS

KD ameliorates HFD-induced adiposity and fatty liver

To investigate the effect of KD on fatty liver in HFD-induced obese mice, we compared the metabolic characteristics of CD, HFD, and KD groups. After 16 weeks of diet intervention (Fig. 1A), the body weight (31.86 ± 3.12 vs 36.44 ± 1.74 g; $P < 0.05$), fasting blood glucose (7.82 ± 0.76 vs 10.64 ± 0.33 mmol/L; $P < 0.001$), and fat mass-to-body weight ratio ($16.12\% \pm 3.54\%$ vs $24.89\% \pm 4.26\%$; $P < 0.05$) of mice in the KD group were significantly lower than those in the HFD group (Fig. 1B–D) despite higher energy intake (14.75 ± 0.94 vs 13.66 ± 0.30 kcal/d; $P < 0.05$) (Fig. 1E). Although we did not observe a beneficial effect on glucose tolerance, insulin resistance was remarkably improved, with lower serum insulin levels in the KD group (Fig. 1F–H). Remarkable decrease in circulating lipid profiles, including triglyceride (86.71 ± 5.30 vs 153.63 ± 19.51 mg/dL; $P < 0.05$), total cholesterol (28.36 ± 7.81 vs 49.33 ± 9.83 mg/dL; $P < 0.01$), and free fatty acid (0.56 ± 0.06 vs 0.77 ± 0.06 mmol/L; $P < 0.01$), were also found in the KD group (Fig. 1I–K). As the liver is one of the major organs contributing to lipid metabolism, we further

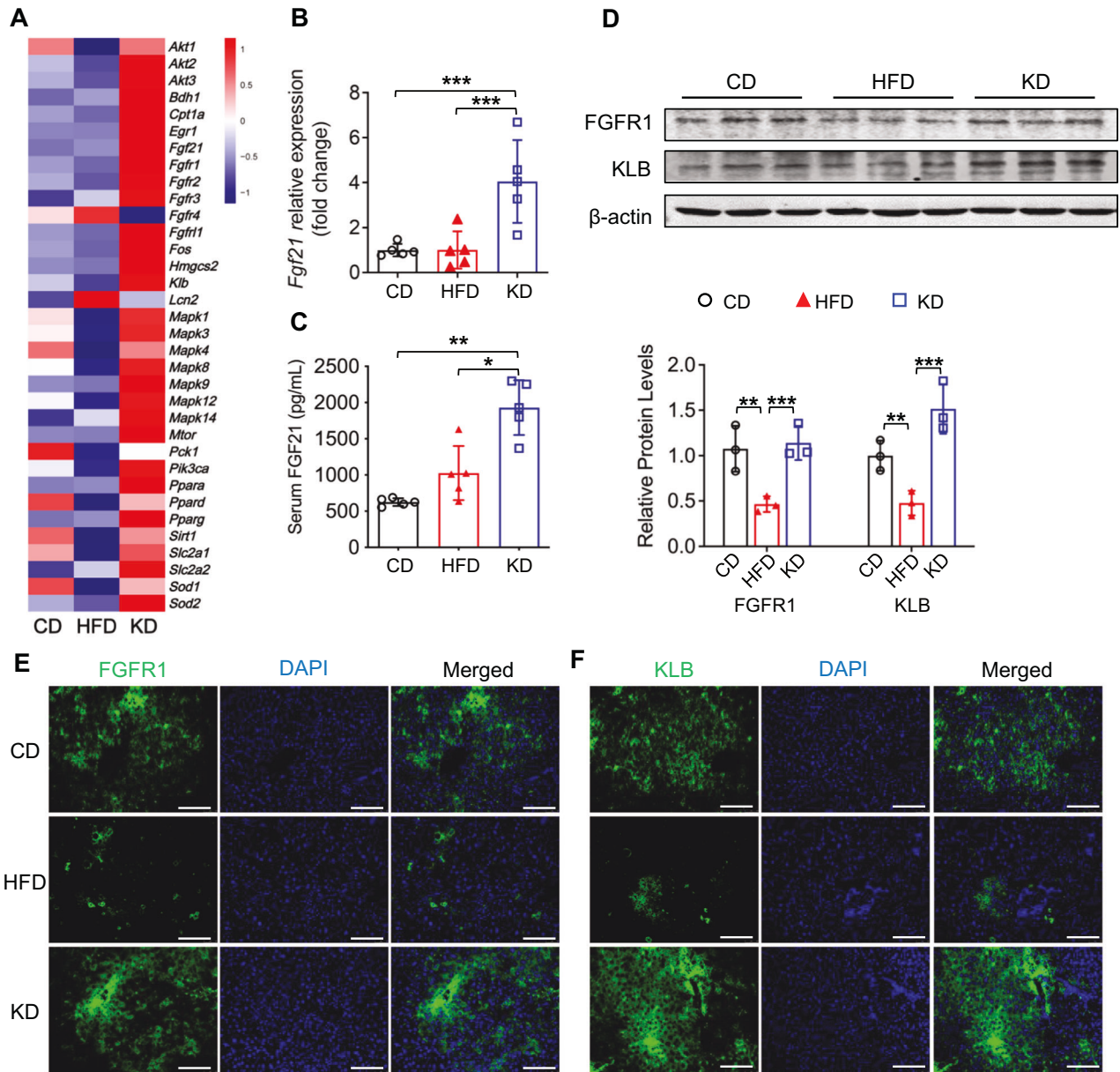


Fig. 3 KD upregulates FGF21 and activates FGF21-KLB signaling in the liver. **A** Heatmap showing expression of genes related to FGF21 signaling in the liver. Blue, downregulation; red, upregulation. **B** mRNA expression of *Fgf21* in the liver. **C** FGF21 levels in circulating. **D** FGFR1 and KLB expression in the liver. **E, F** Immunofluorescence staining of albumin, FGFR1 and KLB in the liver. Green, FGFR1 **E** and KLB **F**; blue, DAPI (magnification 200 \times , scale bar, 100 μ m). FGF21, fibroblast growth factor 21; FGFR1, fibroblast growth factor receptor 1; KLB, β -klotho. $n = 5$ mice per group. * $P < 0.05$; ** $P < 0.01$; *** $P < 0.001$.

characterized the liver weight and histological sections of mice fed with different diets. KD reduced the HFD-increased liver weight (0.96 ± 0.06 vs 1.22 ± 0.10 g; $P < 0.001$) (Fig. 1L), implying that KD might alleviate HFD-induced hepatic steatosis. The histological results directly showed that KD reduced the HFD-induced lipid accumulation in the liver (Fig. 1M, N). In summary, KD alleviated HFD-induced obesity and partly ameliorated obesity-related metabolic disorders, including hepatic steatosis.

KD activates hepatic fatty acid oxidation and suppresses lipogenesis

Next, we measured hepatic lipid levels and lipid metabolism gene expression. Consistently, we found that KD remarkably reduced liver triglyceride (30.99 ± 3.48 vs 156.01 ± 45.47 mg/g; $P < 0.001$) and total cholesterol content (2.43 ± 0.51 vs 9.03 ± 0.39 mg/g; $P < 0.001$)

compared with HFD (Fig. 2A, B). Using multiple experimental approaches, we demonstrated that the positive lipid metabolic effect of KD was associated with the significant downregulation of lipogenic genes (*Fasn* and *Scd1*) and upregulation of key genes in fatty acid oxidation (*Cpt1a* and *Acox1*) compared with HFD both in transcriptional and translational levels (Fig. 2C–H). Taken together, these results indicated that KD alleviated HFD-induced hepatic steatosis by suppressing lipogenesis and promoting lipid oxidation.

KD upregulates FGF21 and activates FGF21-KLB signaling in the liver

To uncover the mechanisms underlying the improvement in hepatic steatosis by a KD, we performed RNA-Seq analysis on mouse livers and found that the mRNA expression profile of *Fgf21* signaling was significantly upregulated, especially *Fgf21*, *Klb*, and

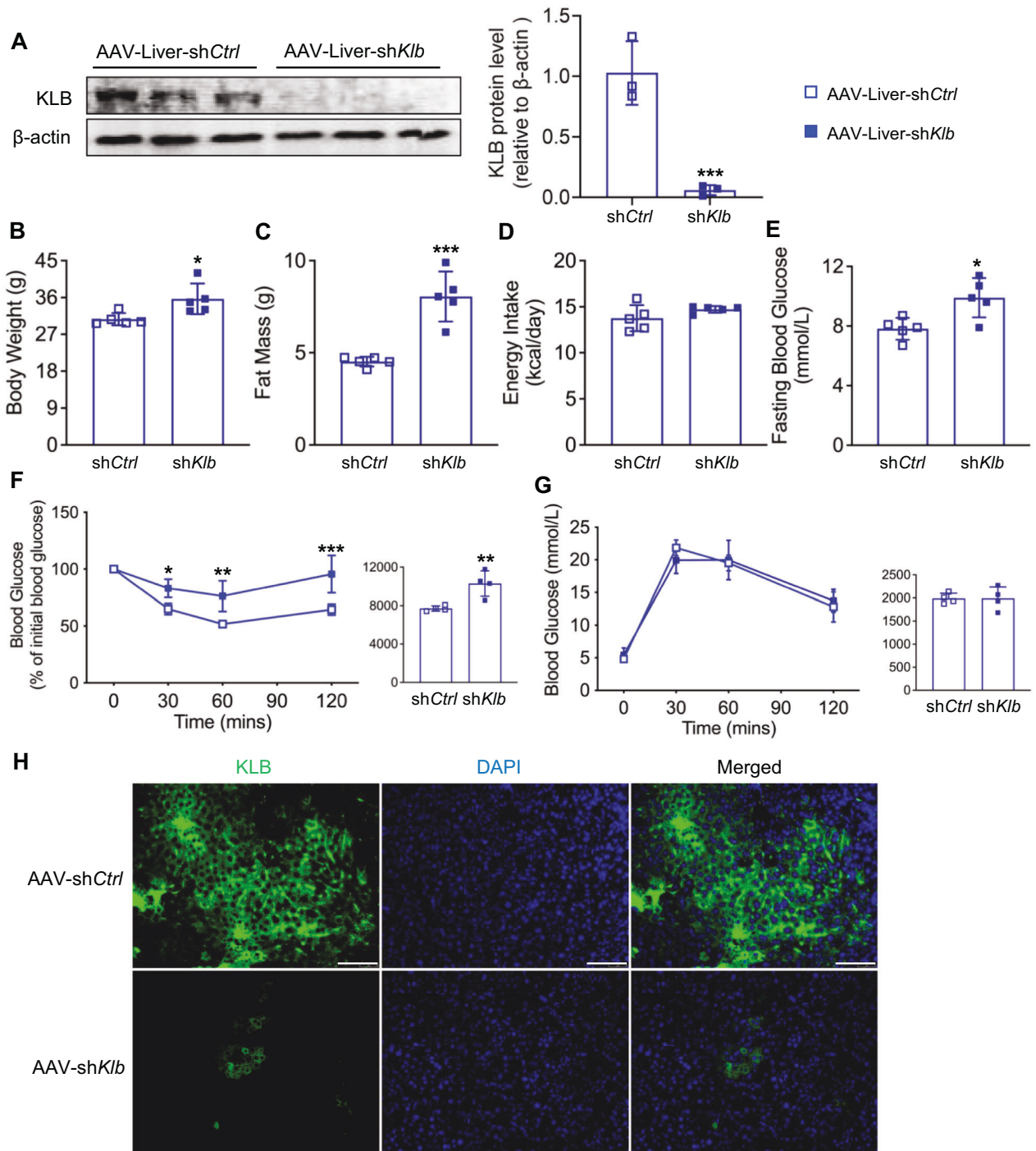


Fig. 4 Liver KLB knockdown diminishes the effect of KD on ameliorating metabolic disorders. **A** Liver KLB expression. **B** Body weight. **C** Body fat mass. **D** Energy intake. **E** Fasting blood glucose. **F** Intraperitoneal insulin tolerance test. **G** Intraperitoneal glucose tolerance test. **H** Immunofluorescence staining of albumin and KLB in the liver. Green, KLB; blue, DAPI (magnification 200 \times , scale bar, 100 μ m). KLB, β -klotho. $n = 4$ –5 mice per group. * $P < 0.05$; ** $P < 0.01$; *** $P < 0.001$.

Fgfr1 (Fig. 3A). The downstream genes of *Fgf21* signaling, including *Egr1* and *c-Fos*, showed the same expression trend (Fig. 3A). We further validated the results using qPCR, ELISA, western blotting, and histological analyses of mouse livers. Consistent with the RNA-Seq data, serum FGF21 levels and expression of FGFR1 and KLB were increased in the KD group (Fig. 3B–F). These data suggested a regulatory effect of KD on serum FGF21 levels and FGF21 signaling activation.

Liver KLB knockdown diminishes the effect of KD on ameliorating metabolic disorders

To further confirm the role of liver FGF21 signaling in the improvement of metabolic disorders induced by a KD, we generated liver KLB knockdown mice using AAV injection. Knockdown efficiency was verified by western blotting and immunofluorescence staining (Fig. 4A, H). Notably, KD-induced improvement of overweight (30.72 ± 1.49 vs 35.68 ± 3.74 g; $P < 0.05$), excessive body fat

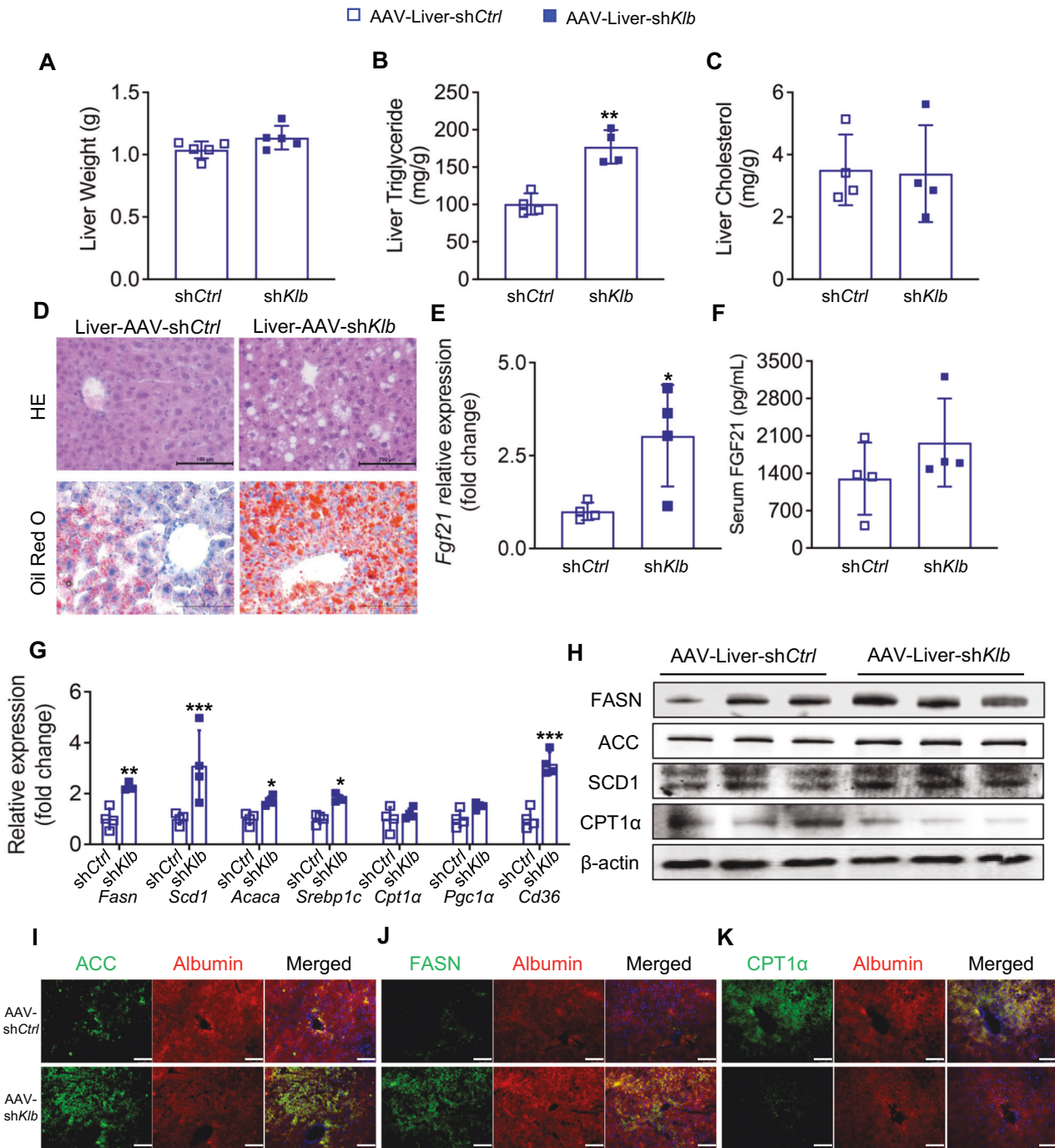


Fig. 5 KD-ameliorated hepatic steatosis is dependent on liver FGF21-KLB signaling. **A** Liver weight. **B** Liver triglyceride level. **C** Liver cholesterol level. **D** Hematoxylin and eosin and Oil Red O staining of the liver. **E** Liver *Fgf21* expression. **F** Serum FGF21 level. **G** Expression of genes related to lipid metabolism in the liver. **H** Lipid metabolism related protein levels in the liver. **I–K** Immunofluorescence staining of albumin, ACC, FASN, and CPT1α in the liver. Green, ACC I, FASN J, and CPT1α K; red, albumin; blue, DAPI (magnification 200×, scale bar, 100 μm). FGF21, fibroblast growth factor 21; *Fasn*, fatty acid synthase; *Acaca*, acetyl-CoA carboxylase; *Srebp1c*, sterol regulatory element binding protein 1c; *Pgc1α*, peroxisome proliferator-activated receptor gamma coactivator 1-alpha; SCD1, stearyl-coenzyme A desaturase 1. $n = 4-5$ mice per group. * $P < 0.05$; ** $P < 0.01$; *** $P < 0.001$.

(4.52 ± 0.26 vs 8.06 ± 1.36 g; $P < 0.001$), hyperglycemia (7.82 ± 0.73 vs 9.90 ± 1.32 mmol/L; $P < 0.05$), and insulin resistance were diminished after KLB knockdown in mouse livers (Fig. 4B, C and E, F). However, liver KLB deficiency had no influence on food intake (13.76 ± 1.42 vs 14.72 ± 0.36 kcal/d; $P > 0.05$) and glucose tolerance (Fig. 4D, G). These data revealed the indispensable role of liver KLB in the beneficial hepatic metabolic effects of KD.

KD-ameliorated hepatic steatosis is dependent on liver FGF21-KLB signaling

Although there was no difference in liver weight (1.04 ± 0.07 vs 1.14 ± 0.09 g; $P > 0.05$) and total cholesterol content (3.51 ± 1.13 vs 3.39 ± 1.56 mg/g; $P > 0.05$) between normal and KLB knock-down mice, liver triglyceride quantification (100.62 ± 14.12 vs 177.07 ± 22.41 mg/g; $P < 0.05$) and histological analysis showed

that liver KLB knockdown diminished the beneficial effect of KD on alleviating hepatic lipid accumulation (Fig. 5A–D). Although *Fgf21* expression in the liver was upregulated by KLB deficiency, circulating FGF21 levels were unaffected in these mice (Fig. 5E, F). We further examined the transcriptional and translational levels of key hepatic metabolic factors. The results showed that lipogenic genes (*Fasn*, *Scd1*, *Acaca*, and *Srebp1c*) and *Cd36*, which are related to lipid uptake, were significantly upregulated in the livers of KLB knockdown mice without affecting genes related to fatty acid oxidation (Fig. 5G). Similarly, the protein expression of lipogenic proteins (FASN, ACC, and SCD1) was higher, whereas CPT1 α was lower in liver KLB knockdown mice (Fig. 5H–K). Thus, liver KLB knockdown impaired the beneficial effect of KD on ameliorating hepatic steatosis, particularly by suppressing lipogenesis, suggesting that FGF21–KLB signaling might be critical for KD-ameliorated hepatic steatosis.

DISCUSSION

NAFLD is a complex disease for which diet and lifestyle interventions are the main treatment options. Studies have suggested that a KD may ameliorate hepatic steatosis. This study aims to delve deeper into the influence of KD on FGF21 expression and its responsiveness through the FGF21–KLB pathway, underscoring the pivotal role of FGF21–KLB signaling in mediating the KD's beneficial effects on hepatic steatosis.

Extensive validation in rodent models has established the therapeutic potential of FGF21 for obesity and related metabolic disorders [15, 16, 18–21, 31, 32]. Consistent with prior research, our observations indicated a significant increase in liver FGF21 expression in KD mice [23, 24]. However, it's noteworthy that heightened endogenous FGF21 levels have been documented in people with obesity, NAFLD, and diabetes [33–35], indicative of a state of FGF21 resistance [36]. This resistance may diminish the sensitivity to endogenous FGF21, potentially limiting the efficacy of low-dose FGF21 treatment [37]. Therefore, enhancing FGF21 sensitivity becomes crucial for achieving its therapeutic effects.

Our investigation revealed that KD elevated hepatic expression levels of KLB and FGFR1 and that KLB plays a critical role in enhancing the binding affinity of FGFR proteins for FGF21. Loss of KLB diminishes these receptors' responsiveness to FGF21 [26]. Aligned with prior studies [17, 19, 31], we validated that KD upregulates FGF21 and KLB expression, leading to a reduction in hepatic steatosis. Utilizing a liver-specific KLB knockdown mouse model, we further confirmed this association, highlighting the profound impact of KLB deficiency in limiting KD's improvement of hepatic steatosis, suggesting the indispensability of the liver FGF21–KLB pathway.

In the context of liver metabolism, ACC and FASN proteins play pivotal roles in lipogenesis and are increased during NAFLD progression. Clinical and preclinical studies targeting these proteins have shown significant reductions in hepatic steatosis and NAFLD resolution [38–40]. Our current study demonstrates that KD treatment downregulates both ACC1 and FASN expression at transcript and protein levels while elevating CPT1 α expression, which is crucial for β -oxidation in lipid metabolism. However, in the hepatic KLB knockdown mouse model, KD's effect on the alteration of these genes was nullified. These results suggest that KD suppresses liver lipogenesis, enhances β -oxidation, and ameliorates hepatic steatosis, contingent upon FGF21–KLB signaling. Additionally, we noted that the loss of FGF21–KLB signaling attenuated KD's effect on decreasing hepatic triglyceride content, but not total cholesterol levels.

Understanding the factors bridging KD and FGF21 remains under exploration. Hepatic FGF21 has been linked as a downstream of peroxisome proliferator-activated receptor alpha (PPAR α) [23, 41], activating transcription factor 4 (ATF4) [42] and SIRT1 [43]. KD failed to increase FGF21 expression in PPAR α -

deficient mice [23], indicating a potential connection between KD and FGF21–KLB signaling. Additionally, the increase in circulating ketones induced by the KD might contribute to its ameliorative effects on metabolic disorders. For example, *Hmgcs2* and *Bdh1*, which are involved in ketogenesis [44], are upregulated by KD, suggesting a novel pathway for KD-ameliorated metabolic disorders. Further research is warranted to explore potential KD-related strategies for the treatment of NAFLD.

However, our study observed limitations of KD. The results of the glucose tolerance test revealed hyperglycemia in the KD group upon glucose stimulation, suggesting potential side effects on β -cell function. Previous research also indicates that KD causes glucose intolerance after 5 weeks and reduces β -cell mass after 22 weeks [45]. Nonetheless, this study contributes to comprehending the mechanisms underlying KD's therapeutic effects on metabolic disorders, particularly on NAFLD.

By elucidating the crucial involvement of the FGF21–KLB pathway in KD's beneficial effects on hepatic steatosis, this study sheds light on the intricate interplay among dietary interventions, metabolic signaling pathways, and hepatic lipid metabolism. These findings hold potential for guiding future research and development of targeted therapeutic approaches for managing NAFLD and related conditions.

DATA AVAILABILITY

All data generated or analyzed during this study are included in this published article and its supplementary information files.

REFERENCES

- Riazi K, Azhari H, Charette JH, Underwood FE, King JA, Afshar EE, et al. The prevalence and incidence of NAFLD worldwide: a systematic review and meta-analysis. *Lancet Gastroenterol Hepatol*. 2022;7:851–61. [https://doi.org/10.1016/S2468-1253\(22\)00165-0](https://doi.org/10.1016/S2468-1253(22)00165-0)
- Romero-Gómez M, Zelber-Sagi S, Trenell M. Treatment of NAFLD with diet, physical activity and exercise. *J Hepatol*. 2017;67:829–46. <https://doi.org/10.1016/j.jhep.2017.05.016>
- Sampaio LP. Ketogenic diet for epilepsy treatment. *Arq Neuropsiquiatr*. 2016;74:842–8. <https://doi.org/10.1590/0004-282X20160116>
- Mardinoglu A, Wu H, Bjornson E, Zhang C, Hakkarainen A, Rasanen SM, et al. An integrated understanding of the rapid metabolic benefits of a carbohydrate-restricted diet on hepatic steatosis in humans. *Cell Metab*. 2018;27:559–71.e5. <https://doi.org/10.1016/j.cmet.2018.01.005>
- Cunha GM, Guzman G, De Mello LLC, Trein B, Spina LDC, Bussade I, et al. Efficacy of a 2-month very low-calorie ketogenic diet (VLCKD) compared to a standard low-calorie diet in reducing visceral and liver fat accumulation in patients with obesity. *Front Endocrinol*. 2020;11:607. <https://doi.org/10.3389/fendo.2020.00607>
- Li J, Bai WP, Jiang B, Bai LR, Gu B, Yan SX, et al. Ketogenic diet in women with polycystic ovary syndrome and liver dysfunction who are obese: a randomized, open-label, parallel-group, controlled pilot trial. *J Obstet Gynaecol Res*. 2021;47:1145–52. <https://doi.org/10.1111/jog.14650>
- Kennedy AR, Pissios P, Otu H, Roberson R, Xue B, Asakura K, et al. A high-fat, ketogenic diet induces a unique metabolic state in mice. *Am J Physiol Endocrinol Metab*. 2007;292:E1724–39. <https://doi.org/10.1152/ajpendo.00717.2006>
- Holland AM, Kephart WC, Mumford PW, Mobley CB, Lowery RP, Shake JJ, et al. Effects of a ketogenic diet on adipose tissue, liver, and serum biomarkers in sedentary rats and rats that exercised via resisted voluntary wheel running. *Am J Physiol-Regul Integr Comp Physiol*. 2016;311:R337–R51. <https://doi.org/10.1152/ajpregu.00156.2016>
- Newman JC, Covarrubias AJ, Zhao M, Yu X, Gut P, Ng CP, et al. Ketogenic diet reduces midlife mortality and improves memory in aging mice. *Cell Metab*. 2017;26:547–57.e8. <https://doi.org/10.1016/j.cmet.2017.08.004>
- Roberts MN, Wallace MA, Tomilov AA, Zhou ZY, Marcotte GR, Tran D, et al. A ketogenic diet extends longevity and healthspan in adult mice. *Cell Metab*. 2017;26:539. <https://doi.org/10.1016/j.cmet.2017.08.005>
- Cao H, Cai Q, Guo W, Su Q, Qin H, Wang T, et al. Malonylation of Acetyl-CoA carboxylase 1 promotes hepatic steatosis and is attenuated by ketogenic diet in NAFLD. *Cell Rep*. 2023;42:112319. <https://doi.org/10.1016/j.celrep.2023.112319>
- Srivastava S, Baxa U, Niu G, Chen X, Veech RL. A ketogenic diet increases brown adipose tissue mitochondrial proteins and UCP1 levels in mice. *IUBMB Life*. 2013;65:58–66. <https://doi.org/10.1002/iub.1102>

13. Goldberg EL, Shchukina I, Asher JL, Sidorov S, Artyomov MN, Dixit VD. Ketogenesis activates metabolically protective $\gamma\delta$ T cells in visceral adipose tissue. *Nature Metabolism*. 2020;2:50–61. <https://doi.org/10.1038/s42255-019-0160-6>
14. Fisher FM, Maratos-Flier E. Understanding the Physiology of FGF21. *Annu Rev Physiol*. 2016;78:223–41. <https://doi.org/10.1146/annurev-physiol-021115-105339>
15. Kharitonov A, Shiyanova TL, Koester A, Ford AM, Micanovic R, Galbreath EJ, et al. FGF-21 as a novel metabolic regulator. *J Clin Invest*. 2005;115:1627–35. <https://doi.org/10.1172/Jci23606>
16. Coskun T, Bina HA, Schneider MA, Dunbar JD, Hu CC, Chen Y, et al. Fibroblast growth factor 21 corrects obesity in mice. *Endocrinology*. 2008;149:6018–27. <https://doi.org/10.1210/en.2008-0816>
17. Xu J, Lloyd DJ, Hale C, Stanislaus S, Chen M, Sivits G, et al. Fibroblast growth factor 21 reverses hepatic steatosis, increases energy expenditure, and improves insulin sensitivity in diet-induced obese mice. *Diabetes*. 2009;58:250–9. <https://doi.org/10.2337/db08-0392>
18. Fisher FM, Kleiner S, Douris N, Fox EC, Mepani RJ, Verdeguer F, et al. FGF21 regulates PGC-1 and browning of white adipose tissues in adaptive thermogenesis. *Genes Dev*. 2012;26:271–81. <https://doi.org/10.1101/gad.177857.111>
19. Gao M, Ma Y, Cui R, Liu D. Hydrodynamic delivery of FGF21 gene alleviates obesity and fatty liver in mice fed a high-fat diet. *J Control Release*. 2014;185:1–11. <https://doi.org/10.1016/j.jconrel.2014.03.047>
20. Gong Q, Hu Z, Zhang F, Cui A, Chen X, Jiang H, et al. Fibroblast growth factor 21 improves hepatic insulin sensitivity by inhibiting mammalian target of rapamycin complex 1 in mice. *Hepatology*. 2016;64:425–38. <https://doi.org/10.1002/hep.28523>
21. Schlein C, Talukdar S, Heine M, Fischer AW, Krott LM, Nilsson SK, et al. FGF21 lowers plasma triglycerides by accelerating lipoprotein catabolism in white and brown adipose tissues. *Cell Metab*. 2016;23:441–53. <https://doi.org/10.1016/j.cmet.2016.01.006>
22. Harrison SA, Ruane PJ, Freilich BL, Neff G, Patil R, Behling CA, et al. Efruxifermin in non-alcoholic steatohepatitis: a randomized, double-blind, placebo-controlled, phase 2a trial. *Nat Med*. 2021;27:1262–71. <https://doi.org/10.1038/s41591-021-01425-3>
23. Badman MK, Pissios P, Kennedy AR, Koukos G, Flier JS, Maratos-Flier E. Hepatic fibroblast growth factor 21 is regulated by PPAR α and is a key mediator of hepatic lipid metabolism in ketotic states. *Cell Metab*. 2007;5:426–37. <https://doi.org/10.1016/j.cmet.2007.05.002>
24. Song P, Zechner C, Hernandez G, Canovas J, Xie Y, Sondhi V, et al. The hormone FGF21 stimulates water drinking in response to ketogenic diet and alcohol. *Cell Metab*. 2018;27:1338–47.e4. <https://doi.org/10.1016/j.cmet.2018.04.001>
25. Badman MK, Koester A, Flier JS, Kharitonov A, Maratos-Flier E. Fibroblast growth factor 21-deficient mice demonstrate impaired adaptation to ketosis. *Endocrinology*. 2009;150:4931–40. <https://doi.org/10.1210/en.2009-0532>
26. Kurosu H, Choi M, Ogawa Y, Dickson AS, Goetz R, Eliseenkova AV, et al. Tissue-specific expression of betaKlotho and fibroblast growth factor (FGF) receptor isoforms determines metabolic activity of FGF19 and FGF21. *J Biol Chem*. 2007;282:26687–95. <https://doi.org/10.1074/jbc.M704165200>
27. Ogawa Y, Kurosu H, Yamamoto M, Nandi A, Rosenblatt KP, Goetz R, et al. BetaKlotho is required for metabolic activity of fibroblast growth factor 21. *Proc Natl Acad Sci USA*. 2007;104:7432–7. <https://doi.org/10.1073/pnas.0701600104>
28. Geng L, Liao B, Jin L, Huang Z, Triggle CR, Ding H, et al. Exercise alleviates obesity-induced metabolic dysfunction via enhancing FGF21 sensitivity in adipose tissues. *Cell Rep*. 2019;26:2738–52.e4. <https://doi.org/10.1016/j.celrep.2019.02.014>
29. Wang SW, Sheng H, Bai YF, Weng YY, Fan XY, Lou LJ, et al. Neohesperidin enhances PGC-1 α -mediated mitochondrial biogenesis and alleviates hepatic steatosis in high fat diet fed mice. *Nutr Diabetes*. 2020;10:27. <https://doi.org/10.1038/s41387-020-00130-3>
30. Xu F, Burk D, Gao Z, Yin J, Zhang X, Weng J, et al. Angiogenic deficiency and adipose tissue dysfunction are associated with macrophage malfunction in SIRT1 $^{-/-}$ mice. *Endocrinology*. 2012;153:1706–16. <https://doi.org/10.1210/en.2011-1667>
31. Lin Z, Pan X, Wu F, Ye D, Zhang Y, Wang Y, et al. Fibroblast growth factor 21 prevents atherosclerosis by suppression of hepatic sterol regulatory element-binding protein-2 and induction of adiponectin in mice. *Circulation*. 2015;131:1861–71. <https://doi.org/10.1161/CIRCULATIONAHA.115.015308>
32. Potthoff MJ, Inagaki T, Satapati S, Ding X, He T, Goetz R, et al. FGF21 induces PGC-1 α and regulates carbohydrate and fatty acid metabolism during the adaptive starvation response. *Proc Natl Acad Sci USA*. 2009;106:10853–8. <https://doi.org/10.1073/pnas.0904187106>
33. Chavez AO, Molina-Carrion M, Abdul-Ghani MA, Folli F, DeFronzo RA, Tripathy D. Circulating fibroblast growth factor-21 is elevated in impaired glucose tolerance and type 2 diabetes and correlates with muscle and hepatic insulin resistance. *Diabetes Care*. 2009;32:1542–6. <https://doi.org/10.2337/dc09-0684>
34. Dushay J, Chui PC, Gopalakrishnan GS, Varela-Rey M, Crawley M, Fisher FM, et al. Increased fibroblast growth factor 21 in obesity and nonalcoholic fatty liver disease. *Gastroenterology*. 2010;139:456–63. <https://doi.org/10.1053/j.gastro.2010.04.054>
35. Li H, Fang Q, Gao F, Fan J, Zhou J, Wang X, et al. Fibroblast growth factor 21 levels are increased in nonalcoholic fatty liver disease patients and are correlated with hepatic triglyceride. *J Hepatol*. 2010;53:934–40. <https://doi.org/10.1016/j.jhep.2010.05.018>
36. Fisher FM, Chui PC, Antonellis PJ, Bina HA, Kharitonov A, Flier JS, et al. Obesity Is a Fibroblast Growth Factor 21 (FGF21)-Resistant State. *Diabetes*. 2010;59:2781–9. <https://doi.org/10.2337/db10-0193>
37. Liu Q, Wang S, Wei M, Huang X, Cheng Y, Shao Y, et al. Improved FGF21 Sensitivity and Restored FGF21 Signaling Pathway in High-Fat Diet/Streptozotocin-Induced Diabetic Rats After Duodenal-jejunal Bypass and Sleeve Gastrectomy. *Front Endocrinol (Lausanne)*. 2019;10:566. <https://doi.org/10.3389/fendo.2019.00566>
38. Goedeke L, Bates J, Vatner DF, Perry RJ, Wang T, Ramirez R, et al. Acetyl-CoA Carboxylase Inhibition Reverses NAFLD and Hepatic Insulin Resistance but Promotes Hypertriglyceridemia in Rodents. *Hepatology*. 2018;68:2197–211. <https://doi.org/10.1002/hep.30097>
39. Lawitz EJ, Coste A, Poordad F, Alkhoury N, Loo N, McColgan BJ, et al. Acetyl-CoA carboxylase inhibitor GS-0976 for 12 weeks reduces hepatic de novo lipogenesis and steatosis in patients with nonalcoholic steatohepatitis. *Clin Gastroenterol Hepatol*. 2018;16:1983–91.e3. <https://doi.org/10.1016/j.cgh.2018.04.042>
40. Syed Abdul MM, Parks EJ, Gaballah AH, Bingham K, Hammoud GM, Kemble G, et al. First-in-class fatty acid synthase inhibitor TVB-2640 reduces hepatic de novo lipogenesis in males with metabolic abnormalities. *Hepatology*. 2019;72:103–18. <https://doi.org/10.1002/hep.31000>
41. Lundåsen T, Hunt MC, Nilsson L-M, Sanyal S, Angelin B, Alexson SEH, et al. PPAR α is a key regulator of hepatic FGF21. *Biochem Biophys Res Commun*. 2007;360:437–40. <https://doi.org/10.1016/j.bbrc.2007.06.068>
42. De Sousa-Coelho AL, Relat J, Hondares E, Perez-Marti A, Ribas F, Villarroya F, et al. FGF21 mediates the lipid metabolism response to amino acid starvation. *J Lipid Res*. 2013;54:1786–97. <https://doi.org/10.1194/jlr.M033415>
43. Li Y, Wong K, Giles A, Jiang J, Lee JW, Adams AC, et al. Hepatic SIRT1 attenuates hepatic steatosis and controls energy balance in mice by inducing fibroblast growth factor 21. *Gastroenterology*. 2014;146:539–49.e7. <https://doi.org/10.1053/j.gastro.2013.10.059>
44. Puchalska P, Crawford PA. Multi-dimensional roles of ketone bodies in fuel metabolism, signaling, and therapeutics. *Cell Metab*. 2017;25:262–84. <https://doi.org/10.1016/j.cmet.2016.12.022>
45. Ellenbroek JH, van Dijk L, Töns HA, Rabelink TJ, Carlotti F, Ballieux BEPB, et al. Long-term ketogenic diet causes glucose intolerance and reduced β - and α -cell mass but no weight loss in mice. *Am J Physiol-Endocrinol Metab*. 2014;306:E552–E8. <https://doi.org/10.1152/ajpendo.00453.2013>

ACKNOWLEDGEMENTS

This work was supported by National Natural Science Foundation of China Grants (nos. 82270942, 81970741, and 82300956), the Local Innovative and Research Teams Projects of Guangdong Pearl River Talents Program (2017BT015131), the Science and Technology Program of Guangzhou (202102010229).

AUTHOR CONTRIBUTIONS

WG and HC performed the experiments, analyzed the research data, and wrote the manuscript. YS, WL, WW, and LC, contributed to animal experiments. MC contributed to the study design. FX designed the study, analyzed the research data, revised the manuscript, and approved the submitted version. All the authors approved the final manuscript.

COMPETING INTERESTS

The authors declare no competing interests.

ADDITIONAL INFORMATION

Supplementary information The online version contains supplementary material available at <https://doi.org/10.1038/s41387-024-00277-3>.

Correspondence and requests for materials should be addressed to Fen Xu.

Reprints and permission information is available at <http://www.nature.com/reprints>

Publisher's note Springer Nature remains neutral with regard to jurisdictional claims in published maps and institutional affiliations.



Open Access This article is licensed under a Creative Commons Attribution 4.0 International License, which permits use, sharing, adaptation, distribution and reproduction in any medium or format, as long as you give appropriate credit to the original author(s) and the source, provide a link to the Creative Commons licence, and indicate if changes were made. The images or other third party material in this article are included in the article's Creative Commons licence, unless indicated otherwise in a credit line to the material. If material is not included in the article's Creative Commons licence and your intended use is not permitted by statutory regulation or exceeds the permitted use, you will need to obtain permission directly from the copyright holder. To view a copy of this licence, visit <http://creativecommons.org/licenses/by/4.0/>.

© The Author(s) 2024